RSC Advances

PAPER

View Article Online
View Journal | View Issue

Cite this: *RSC Adv.*, 2022, **12**, 24456

The efficient and green synthesis of biodiesel from crude oil without degumming catalyzed by sodium carbonate supported MoS_2†

Tiantian Zhang,[ab] Binglin Li,[a] Haining Li,[a] Yuanyuan Liu,[c] Jiachen Li,[d] Binxia Zhao,[d] Xiaoli Zhang *[a] and Jiao Wang*[e]

Received 7th July 2022
Accepted 14th August 2022

DOI: 10.1039/d2ra04198g

rsc.li/rsc-advances

The transesterification of lecithin with methanol catalyzed by 23 kinds of alkaline salts was investigated for the preparation of biodiesel. Sodium carbonate was confirmed as the best catalyst due to its excellent catalytic performance, environmental friendliness, and great stability. Next, it was successfully immobilized on the surface of hierarchical nanosheets of MoS_2. The prepared catalyst was characterized *via* XRD, FTIR, SEM, and TEM techniques. After immobilization, the highest specific activity reached 40.58 ± 0.78 U $mg_{Na_2CO_3}^{-1}$, which was 2.43 times higher than that of unsupported Na_2CO_3. Meanwhile, the highest yield reached 99.8%. The excellent performance of the supported catalysts was attributed to a synergistic effect between MoS_2 and the absorbed sodium carbonate. Firstly, sodium carbonate was uniformly dispersed on the surface of MoS_2 to minimize the mass transfer resistance. Secondly, the electron-rich outer layer of MoS_2 promoted the deprotonation of methanol to form methoxy anions. The prepared catalyst was further applied in the transesterification of lecithin-containing triglycerides to prepare fatty acid methyl esters (FAMEs). The experimental results showed that the addition of lecithin would promote the transesterification of triglycerides. The yields of FAMEs were close to 100% in all cases when the lecithin content was increased from 1% to 40%. Hence, this supported sodium carbonate catalyst should be a promising candidate for biodiesel production from crude oil without degumming.

1. Introduction

Vegetable oils, animal fats, and wasting cooking oil (WCO) as renewable resources are materials for biodiesel production.[1,2] Traditionally, biodiesel is a kind of fatty acid methyl/ethyl ester (FAME or FAEE) prepared by the transesterification of oil and methanol/ethanol catalyzed by homogeneous strong bases (NaOH, KOH, or methoxides),[3,4] acids (H_2SO_4)[5] and biocatalysts (lipases).[6] Generally, these oils do not suffer the refining process for their low-cost production and, thus, contain some impurities. Gums, as one of the main impurities, have certain negative effects on the transesterification. They are amphipathic surfactants that easily absorb water to swell, resulting in the side reaction of the saponification of triglycerides in the presence of strong alkaline catalysts. On the one hand, the saponification reaction consumes both the substrate (triglycerides) and catalysts, and on the other hand, the product of the saponification reaction is fatty acid salt. Fatty acid salt is a kind of typical surfactant, which will seriously affect the separation of the products FAME and glycerol, resulting in the loss of the FAME. After the reaction, large amounts of acids need to be consumed to neutralize these homogeneous alkaline catalysts and generate the high-salinity wastewater.[3,7] Therefore, a mild and efficient catalyst should be exploited for the transesterification of crude oils without the prior removal of gums.[8]

Calcium methylate and calcium oxide were employed to prepare biodiesel from phosphatidylcholine and crude oil without degumming. As heterogeneous catalysts, they were easily collected after the reaction.[9] The yields of FAMEs were all above 90%.[10] Next, special attention was paid to the alkaline inorganic salts, because they are cheaper and safer than calcium methoxide and calcium oxide. Malins *et al.* used phosphates and carbonates to catalyze the transesterification of triglyceride with methanol.[11] Although an accepted yield was obtained, its operational stability was unsatisfactory due to a certain solubility of pure alkaline salts in the reaction media.[11] The serious drawback of these alkaline inorganic salts is that they are prone to agglomeration, leading to a very low "effective reaction interface". Any catalyst buried in the center of crystals will not be able to interact with substrates and only plays the role of a backbone. Therefore, the use of pre-

[a]College of Food Science and Engineering, Northwest University, Xi'an 710069, China. E-mail: xlzhang@nwu.edu.cn
[b]College of Chemistry and Chemical Engineering, Longdong University, Qingyang 745000, China
[c]Logistics Group, Northwest University, Xi'an 710069, China
[d]College of Chemical Engineering, Northwest University, Xi'an 710069, China
[e]Biochemistry Center (BZH), Heidelberg University, Heidelberg 69120, Germany. E-mail: jiao.wang@bioquant.uni-heidelberg.de

† Electronic supplementary information (ESI) available. See https://doi.org/10.1039/d2ra04198g

existing solids, instead of the "non-active" core of alkaline inorganic salts, should be the most advantageous solution to minimize diffusional resistance. Britton *et al.* employed silica and alumina as supports for the loading of phosphate and carbonate salts.[12] Martínez-Klimov *et al.* supported sodium carbonate on sodium titanate nanotubes for the transesterification of soybean oil with methanol.[13] Although many works have focused on the transesterification of refined oil (degummed oil), less attention has been paid to the transesterification of phospholipids, which limits the application of alkaline salts in the production of biodiesel from crude oil (without degumming).[14]

In this work, 23 kinds of alkaline salts were employed as catalysts to illustrate the transesterification of phospholipids while preparing biodiesel. The effects of cations and anions of alkaline inorganic salts were comprehensively analyzed. Then, the best candidate was immobilized on hierarchical nanosheets of molybdenum disulfide (MoS_2) with a petal-like structure to maximize the specific activity of catalysts. Interestingly, MoS_2 also showed a certain catalytic activity for the transesterification of phospholipids. Therefore, the superior activity was attributed to the synergistic effect between alkaline inorganic salts and the carrier MoS_2. A possible catalytic mechanism was proposed. The reutilization of the supported catalysts was also investigated. Finally, this synergistic catalyst was applied in the transesterification of lecithin-containing oils to prepare FAMEs.

2. Experimental

2.1 Materials

Lecithin (the content of phosphatidylcholine, PC, ≥50%) was purchased from Merya's Lecithin Co., Ltd. (Beijing, China). The 37 kinds of fatty acid methyl ester standards for analysis were purchased from Sigma-Aldrich Co., Ltd (Norcross, GA). Sodium molybdate dihydrate and thiourea were purchased through Tansoole with 99.9% purity (Adama's band). All 23 kinds of alkaline salts were purchased from Sinopharm Chemical Reagent Co., Ltd. (Shanghai, China). Refined soybean oil was purchased from Yihai Kerry Arawana Holdings Co., Ltd. (Shanghai, China) and used without further purification. All the other reagents used were of analytical grade.

2.2 MoS_2 preparation

MoS_2 hierarchical nanostructures were successfully fabricated *via* a facile hydrothermal process.[15,16] Sodium molybdate ($Na_2MoO_4 \cdot 2H_2O$) was dissolved in 5 mL of deionized water with a concentration of 1 mM; thiourea (CH_4N_2S) was dissolved in 5 mL of deionized water with a concentration of 4 mM. The obtained solutions were mixed for 20 min under vigorous stirring. The mixture was transferred into a 15 mL Teflon-lined stainless-steel autoclave which was properly sealed and placed in an oven for hydrothermal treatment at 220 °C for 24 h. The oven was allowed to cool naturally to room temperature. Subsequently, the resulting black solid was retrieved from the solution by centrifugation, washed with distilled water, followed by washing with ethanol twice, and finally dried at 60 °C overnight.

2.3 Supported catalyst preparation

Catalysts with different Na_2CO_3 loadings were prepared by the impregnation method. One milligram of sodium carbonate was dispersed in 1 mL of deionized water, then MoS_2 (19 mg, 9 mg, 5.7 mg, 4 mg, or 3 mg) was added and stirred under 200 rpm for 3 h at room temperature. The mixture was then dried under 85 °C for 12 h to obtain supported MoS_2 catalysts with different Na_2CO_3 loadings of 5%, 10%, 15%, 20%, and 25%.

2.4 Characterization techniques

Powder X-ray diffraction (XRD) (Rigaku Ultima IV, 10° min^{-1}, Japan) was used to determine the crystal phase of the MoS_2 carrier before and after the support of sodium carbonate. The morphology was investigated *via* scanning electron microscopy (SEM) using a Carl Zeiss SIGMA (ZEISS, Germany) instrument equipped with a field-emission gun operated at 15.0 kV. High-resolution transmission electron microscopy (HRTEM) characterization was performed on a JEOL 2100F electron microscope to monitor the deep morphology. The chemical functional groups of all samples were recorded by Fourier transform infrared (FTIR) spectroscopy (PerkinElmer, America). Specific surface areas were calculated by the Brunauer–Emmett–Teller (BET) method.

2.5 Transesterification of lecithin

Alkaline salts or supported catalysts were added into 20 mL of a methanol solution containing 10 mg of lecithin. The amounts of alkaline salts were all controlled at 0.2 mmol to study the effects of the types of catalysts on the transesterifications, as shown in Table 1. After Na_2CO_3 was confirmed as the best candidate, the amount of Na_2CO_3 was fixed and used as a standard for all supported catalysts, which was 0.0094 mmol (1 mg). The mixture was incubated at different temperatures (room temperature, 40 °C, 50 °C, and 60 °C) at 500 rpm. The reaction mixture was separated by centrifugation. The upper liquid was used to analyze FAMEs by gas chromatography (GC).

2.6 Transesterification of triglycerides containing lecithin

A certain amount of lecithin (1 mg, 10 mg, 20 mg, or 40 mg) was mixed with 100 mg of triglycerides in 20 mL of methanol. Five milligrams of 20% Na_2CO_3 supported MoS_2 were added to start the reaction. The mixture was incubated at 50 °C at 500 rpm. After the transesterification, the mixture was separated by centrifugation. The upper liquid was used to analyze FAMEs by GC.

2.7 Methyl esterification of lecithin and triglycerides

Methyl esterifications of lecithin and triglycerides were carried out for GC analysis according to AOCS standard method 996.01.[17] One milligram of lecithin (or triglycerides) was mixed with 0.5 mL of potassium hydroxide methanol solution with a concentration of 2 M under vigorous shaking for 1 min. The obtained solution was further allowed to stand for 5 min. One milliliter of the chromatographic isooctane was used to extract the FAMEs. The isooctane phase was collected, anhydrous sodium sulfate was added to remove water, then the phase was

Table 1 Yields of FAMEs catalyzed by different salts in the transesterification of phospholipids with methanol[a]

Catalyst	Formula	Yield (%)	Solubility[b]
Potassium phosphate	K_3PO_4	92.2 ± 0.89	IS
Sodium phosphate	Na_3PO_4	80.0 ± 0.76	IS
Dibasic sodium phosphate	Na_2HPO_4	10.7 ± 1.71	IS
Potassium dihydrogen phosphate	KH_2PO_4	—	IS
Sodium dihydrogen phosphate	NaH_2PO_4	—	IS
Sodium carbonate	Na_2CO_3	98.7 ± 1.1	IS
Potassium carbonate	K_2CO_3	85.1 ± 0.93	S
Sodium bicarbonate	$NaHCO_3$	87.3 ± 1.18	IS
Potassium bicarbonate	$KHCO_3$	90.2 ± 1.08	S
Cesium carbonate	Cs_2CO_3	78.4 ± 0.91	S
Magnesium carbonate	$MgCO_3$	2.7 ± 0.62	IS
Calcium carbonate	$CaCO_3$	—	IS
Strontium carbonate	$SrCO_3$	—	IS
Barium carbonate	$BaCO_3$	—	IS
Manganese carbonate	$MnCO_3$	0.8 ± 0.59	IS
Copper carbonate	$CuCO_3$	—	IS
Nickel carbonate	$NiCO_3$	8.6 ± 0.30	IS
Silver carbonate	Ag_2CO_3	—	IS
Ammonium carbonate	$(NH_4)_2CO_3$	10.58 ± 0.84	S
Ammonium bicarbonate	NH_4HCO_3	4.9 ± 0.35	IS
Sodium acetate	CH_3COONa	3.63 ± 0.41	S
Sodium citrate	$C_6H_5Na_3O_7$	7.4 ± 1.03	IS
Sodium aluminate	$NaAlO_2$	86.9 ± 2.48	IS

[a] Reaction conditions: 10 mg of PC dissolved in 20 mL of methanol, 0.2 mmol of catalyst, ambient temperature with a stirring speed of 500 rpm for 23 h. [b] IS means that 10 mg of the target salt is insoluble or slightly soluble in 2 mL of methanol; S means that 10 mg of the target salt is soluble in 2 mL of methanol.

centrifuged at 9000 × *g* for 5 min. The upper liquid was used to analyze the FAMEs by GC.

2.8 GC analysis

A gas chromatograph (GC2030, Shimadzu, Japan) equipped with a flame-ionization detector was used to analyze the contents of FAMEs. The column was SH-Rtx-wax (30 m × 0.25 mm × 0.25 μm). The oven temperature was held at 165 °C for 1 min, then increased to 210 °C at a rate of 6.5 °C min^{-1}, followed by an increase to 220 °C at a rate of 1.5 °C min^{-1}, then maintained for 1 min. The temperatures of the injector and detector were held at 250 °C and 280 °C, respectively. The flow rates of N_2, H_2, and air were 24, 32, and 200 mL min^{-1}.

The yield of FAMEs was normalized as follows:

$$\text{Yield of FAMEs (\%)} = 100\% \times mF_a/mF_t$$

where mF_a is the amount of FAMEs produced by the transesterification reaction and mF_t is the amount of FAMEs theoretically produced by the total substrates, as described in 2.7.

3. Results and discussion

3.1 Transesterification using different alkaline salt catalysts

The main component of the gums is a complex mixture of phospholipids. Therefore, the soybean lecithin was employed as the substrate to demonstrate the transesterification, which is a kind of typical mixture of phospholipids, and widely exists in many oils, such as vegetable oils, animal oils, and waste cooking oils.[18] Lecithin from the soybean is comprised of 35–55% phosphatidylcholine (PC), 14–17% phosphatidylethanolamine (PE), 14–17% phosphatidylinositol (PI) and 5–8% phosphatidic acid (PA).[19,20] The ideal catalyst should convert lecithin completely, meaning that all kinds of phospholipids can participate in the transesterification.

As shown in Table 1, 23 kinds of alkaline salts were tested by the transesterification of lecithin. The yields of FAMEs were measured to evaluate the reaction efficiencies. Firstly, the catalytic properties of phosphates (including hydrogen phosphates and dihydrogen phosphates) were investigated. The results showed that phosphates of potassium and sodium had higher yields of FAMEs, reaching 92.2% and 80.0%, respectively. However, the catalytic activity was significantly reduced when hydrogen phosphate anion was the anion. For example, only a 10.7% yield of FAMEs was obtained when dibasic sodium phosphate was used. Moreover, when the anion was the dihydrogen phosphate anion, the catalytic activity completely disappeared, both for sodium dihydrogen phosphate and potassium dihydrogen phosphate. Next, the catalytic activities of carbonates and bicarbonates were analyzed. The experimental results were similar to those of phosphates. Both potassium carbonate and sodium carbonate exhibited excellent catalytic activities for the transesterification reaction. The yields of FAMEs reached 98.7% and 85.1%, respectively. The yields of FAMEs were slightly reduced when sodium bicarbonate was used, due to the decrease in the basicity. However, the yield of FAMEs catalyzed by potassium bicarbonate was 90.2%, which was higher than that of potassium carbonate, implying the significance of alkaline salt cations. Therefore, the cations of carbonates were replaced to further evaluate their catalytic performances.

As shown in Table 1, only cesium carbonate showed an acceptable yield of FAMEs (78.4%). Coincidentally, three cations (Na, K, and Cs) of carbonates with good catalytic performance all belong to alkali metal elements of group IA elements. Nickel carbonate, magnesium carbonate, and manganese carbonate have very weak catalytic activities, while calcium carbonate, strontium carbonate, silver carbonate, copper carbonate, and barium carbonate did not show any activity for the transesterification reaction. Thus, the catalytic efficiencies of the carbonates corresponding to alkali metals would be greater than others. For alkali metal carbonates, the catalytic performance decreased with their reduction abilities. The properties of ammonium salts are similar to those of alkali metal salts because ammonium and sodium ions are isoelectronic, and the radius of the ammonium ion (143 pm) approximates that of the potassium ion (133 pm). The catalytic performances of ammonium carbonate and ammonium bicarbonate were tested. The results showed only 10.58% and 4.9% yields of FAMEs were obtained. Then, several alkali organic salts, sodium acetate and sodium citrate, were tested, showing weak catalytic activities. It is worth noting that sodium aluminate also had an acceptable yield of FAMEs, reaching 86.9%.

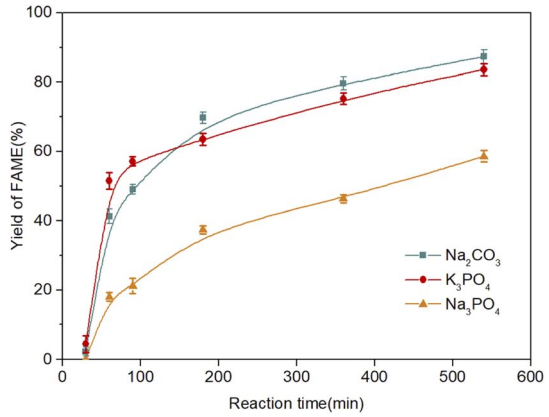

Fig. 1 Effects of catalysts on FAME production from PC. Reaction conditions: 10 mg of PC dissolved in 20 mL of methanol, 5 mg of catalyst, a reaction temperature of 40 °C, a stirring speed of 500 rpm.

The solubility of all used catalysts was investigated in methanol to test their operational stabilities, as shown in Table 1. Unfortunately, potassium carbonate and potassium bicarbonate were completely dissolved in methanol under the specific conditions, which limits the separation of the product and the recovery of the catalyst.[21] In contrast, sodium carbonate and sodium phosphate were insoluble in methanol and glycerol/methanol solution under the experimental conditions, and could be used as heterogeneous catalysts and easily collected by centrifugation after transesterification.[11,21] The ideal catalysts should be cheap, non-toxic, and highly efficient, and exhibit high operational stability. Therefore, sodium carbonate and potassium phosphate were confirmed as the best catalyst candidates, and their catalytic efficiency was intensively studied, as shown in Fig. 1.

Since sodium phosphate has been confirmed as the best candidate catalyst for the transesterification of triglycerides in previous work,[11] it was employed as a reference for comparison with our proposed catalyst. The catalytic performances of sodium carbonate and potassium phosphate were significantly greater than that of sodium phosphate. There is no obvious difference in the catalytic performance between sodium carbonate and potassium phosphate. The hygroscopicity property of catalysts is another essential factor during transesterification. In the presence of water, even a very low water content, the saponification reaction of substrates would be promoted, the catalyst would be consumed, and the difficulty of the downstream recovery of products would be increased. The storage stabilities of potassium phosphate and sodium carbonate were studied. The weight of potassium phosphate increased by more than 60% after being exposed to air for 72 h, while the change of sodium carbonate was negligible (data not shown), which is consistent with the reported literature.[11] Therefore, sodium carbonate is confirmed as the best candidate to catalyze the transesterification reaction.

3.2 Characterization of the supported catalysts

Scanning electron microscopy (SEM) analysis was used to evaluate the morphology of the prepared catalysts. As shown in Fig. 2a, the low magnification SEM image of MoS_2 displayed the hierarchical spherical-like morphology. At high magnification, each hierarchical spherical-like MoS_2 was made up of many smooth curly nanosheets, as shown in Fig. 2b. Particles of sodium carbonate with white outlines uniformly dispersed on the curled nanosheets indicated that the active ingredient, sodium carbonate, was successfully loaded on the surface of MoS_2 without the destruction of the carrier microscopic nanostructures (Fig. 2c and d). However, several obvious aggregations of sodium carbonates attached on the surface of MoS_2 for a 25% sodium carbonate loading are shown in Fig. 2e and f. Some of the voids between the nanosheets of hierarchical spherical-like MoS_2 were blocked and the effective surface of the supported catalyst would be reduced.

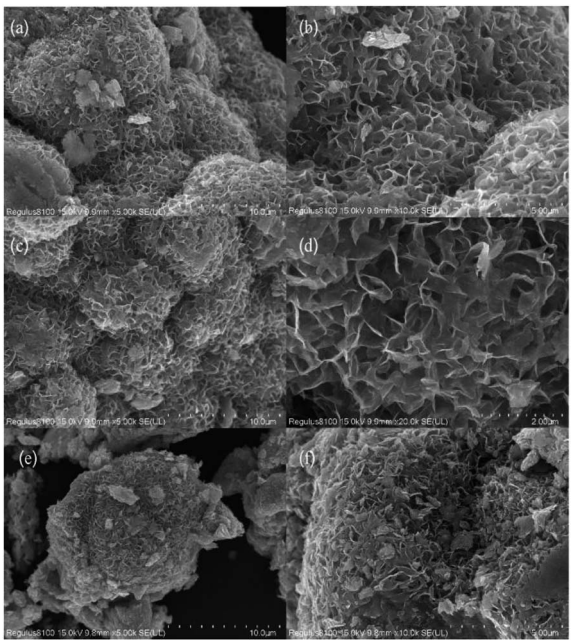

Fig. 2 SEM images of (a) MoS_2 nanostructures at low magnification, (b) MoS_2 nanostructures at high magnification, and supported MoS_2 with (c) 15% Na_2CO_3 at low magnification, (d) 15% Na_2CO_3 at high magnification, (e) 25% Na_2CO_3 at low magnification, and (f) 25% Na_2CO_3 at high magnification.

As shown in Fig. 3a and b, it can be observed that the hierarchical nanostructure of MoS_2 is assembled by the curly nanosheets. Some overlapped black layers and wrinkles were recognized in the TEM images, which was evidence of the larger surface area of the supported MoS_2. The lattice image (Fig. 3c)

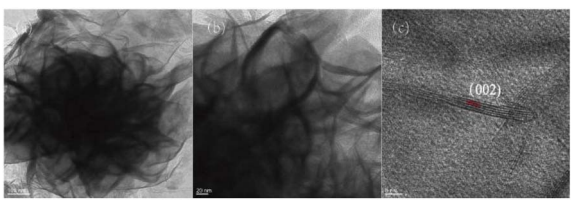

Fig. 3 TEM micrographs of MoS_2 nanostructures at (a) low magnification and (b) high magnification, and (c) a lattice image.

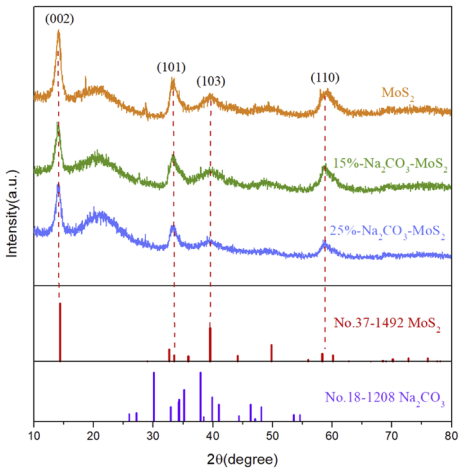

Fig. 4 XRD patterns of MoS_2 and supported MoS_2.

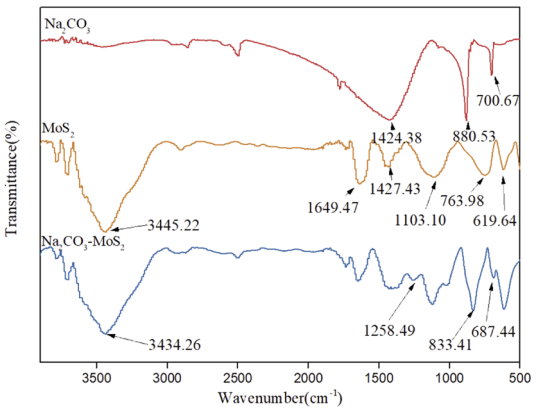

Fig. 5 FT-IR spectra of Na_2CO_3, MoS_2, and supported MoS_2.

indicates that the petal at the twist is made up of around 4 layers with a d value of 6.25 Å, which matches with the available reports of MoS_2.[22]

The XRD patterns of synthesized catalysts are shown in Fig. 4. Sharp diffraction peaks at 14.39°, 33.52°, 39.48°, and 58.86° corresponded to the (002), (101), (103), and (110) crystal planes of MoS_2 (JCPDS no. 37-1492), respectively, with no obvious interference peak. Thus, the great crystallinity of MoS_2 was obtained by the hydrothermal method.[23] After the loading of sodium carbonate, peaks attributed to MoS_2 did not significantly shift, and no peak attributed to sodium carbonate was observed, indicating the stable crystal structure of MoS_2. The overall diffraction peaks were slightly broadened with the loading of sodium carbonates, implying the uniform dispersion of sodium carbonate on the surface of MoS_2.[24]

Fourier transform infrared spectroscopy (FTIR) was employed to elucidate the functional groups of catalysts. As shown in Fig. 5, it included two main infrared absorption peaks of MoS_2.[25] The peak at 619.64 cm^{-1} was related to Mo–S stretching vibration bond and the peak at 763.98 cm^{-1} was related to the S–S stretching vibration bond.[26] The broad signal around 3445 cm^{-1} corresponded to the stretching mode of the interlamellar water molecules in layered MoS_2. For the spectra of supported MoS_2, three new absorption bands were observed. The infrared absorption peak in the frequency range of 687.44 cm^{-1} belonged to the ν_4 vibrational mode, 833.41 cm^{-1} was attributed to the ν_2 vibrational mode, and 1258.49 cm^{-1} was ascribed to the ν_3 vibrational mode of CO_3^{2-} in sodium carbonate, which confirmed the successful immobilization of sodium carbonate on the surface of MoS_2.

Specific surface areas (S_{BET}) were measured by the BET method. The specific surface area of unsupported MoS_2 is 14.82 $m^2\ g^{-1}$, as shown in Table 2. When the loadings of sodium carbonate were 5% and 10%, there is no obvious difference in the S_{BET} of MoS_2. A slight decrease was observed after the incorporation of 15% and 20% of Na_2CO_3. A 20% decrease in the S_{BET} was observed after the incorporation of 25% (11.57 $m^2\ g^{-1}$) of Na_2CO_3, which can be attributed to the serious accumulation of sodium salts above the curled nanosheets, blocking the channel of supports, as shown in Fig. 2f.

3.3 Catalytic activity in the transesterification reaction

Unsupported Na_2CO_3 has a poor specific activity due to the small specific surface area and pore size. The active site buried in the center of the crystals will not be able to contact with the substrates. Therefore, the use of pre-existing solids instead of the "non-active" core of Na_2CO_3 should be the most advantageous solution to uniformly immobilize Na_2CO_3 on the outside surface of carriers and minimize the diffusional resistance. Hierarchical nanosheets of MoS_2 were used as the candidate carrier to disperse sodium carbonate due to their adsorption properties and great stability under alkaline conditions. Moreover, as shown in Fig. 6, the dispersibility of MoS_2 in methanol was excellent. This was mainly due to the unique structure of the hierarchical curly nanosheets, which could not only increase the porosity but also reduce the density of the supports. In addition, the polar surface (the semiconductor property) facilitated the dispersibility of MoS_2 in polar methanol. It was observed in Fig. 6a that sodium carbonate could not reach a uniform dispersion even under vigorous stirring, and parts of it always precipitated on the bottom of the reactor. After standing for 5 min, most sodium carbonate rapidly precipitated. For MoS_2, it was always dispersed well in methanol in both cases. The excellent dispersibility provided the sufficient effective surface between the catalyst and the substrates.

The catalytic performances of the prepared catalysts were evaluated by the transesterification of lecithin with methanol. As shown in Fig. 7, MoS_2 alone showed unneglectable catalytic activity in the transesterification and a 5.7% yield of FAMEs was obtained. However, the catalytic activity of Na_2CO_3 was significantly higher than that of MoS_2. The maximum yield of the former (58.5%) was about ten times higher than that of the latter. Thus, Na_2CO_3 as the main active component was controlled at the same amount in all supporting MoS_2 experiments, as described in Part 2.5. The initial slope and maximum yield should directly reflect the specific activity and maximum reaction rate of the prepared catalysts, as shown in Table 2. The specific activity and maximum yield of unsupported Na_2CO_3

Table 2 Specific surface areas and specific activities of the catalysts

Catalyst	S_{BET}[a] ($m^2\ g^{-1}$)	Specific activity[b] (U $mg_{Na_2CO_3}^{-1}$)	Maximum yield of FAMEs[c] (%)
Na_2CO_3	1.82	11.81 ± 0.56	58.51 ± 1.60
MoS_2	14.82	—	5.72 ± 0.29
5% Na_2CO_3 supported MoS_2	14.61	16.39 ± 0.60	78.52 ± 1.83
10% Na_2CO_3 supported MoS_2	14.36	29.12 ± 0.65	92.24 ± 1.92
15% Na_2CO_3 supported MoS_2	13.79	32.03 ± 0.70	94.46 ± 1.46
20% Na_2CO_3 supported MoS_2	13.18	40.58 ± 0.78	99.82 ± 0.15
25% Na_2CO_3 supported MoS_2	11.57	32.60 ± 0.83	91.13 ± 1.19

[a] Specific surface area (S_{BET}) values were measured *via* the BET method. [b] Specific activities were calculated according to the initial slope of FAMEs within 240 minutes, where U represents ‰ FAMEs min^{-1}. [c] Maximum yield of FAMEs obtained from Fig. 7.

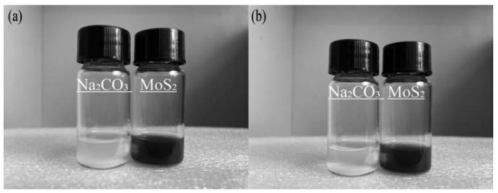

Fig. 6 Dispersibility of sodium carbonate and MoS_2 in methanol (a) after stirring at 500 rpm for 30 min and (b) after standing for another 5 minutes after stirring.

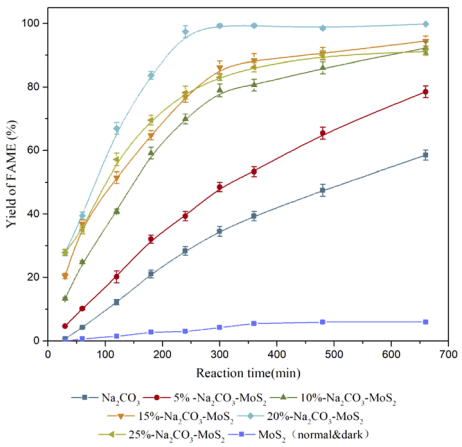

Fig. 7 Yields of FAMEs catalyzed by different loading amounts of supported catalysts. Reaction conditions: 10 mg of PC dissolved in 20 mL of methanol, a catalyst dosage with 1 mg of sodium carbonate and the corresponding mass of the supported catalyst, 50 °C with a stirring speed of 500 rpm.

were 11.81 ± 0.56 U $(mg_{Na_2CO_3})^{-1}$ and 58.51 ± 1.60%, respectively. For the supported catalysts, the specific activity increased from 16.39 ± 0.60 to 40.58 ± 0.78 U $(mg_{Na_2CO_3})^{-1}$ and the maximum yield increased from 78.52 ± 1.83% to 99.82 ± 0.15%, with the sodium carbonate increasing from 5% to 20%. Beyond that, a decrease was observed in the specific activity and maximum yield. Aggregations of sodium carbonate caused by multilayer adsorption on the surface of MoS_2 were formed under high loadings, as shown in Fig. 4f. Therefore, the specific surface area decreased significantly and many active components (Na_2CO_3) were buried in these aggregations, increasing the mass transfer resistance and reducing the reaction efficiency. The optimal loading of Na_2CO_3 was confirmed as 20%.

3.4 Effect of reaction temperature on the transesterification

As shown in Fig. 8, the catalytic performance of 20% Na_2CO_3 supported MoS_2 was evaluated and compared with that of Na_2CO_3 under different temperatures (40 °C, 50 °C, and 60 °C). The results indicated that higher yields of FAMEs were obtained in all cases of supported MoS_2. The lowest yield of FAMEs of supported MoS_2 (92.24 ± 2.19%) was even higher than the highest yield of FAMEs of Na_2CO_3 (81.92 ± 0.86%). The highest yield of FAMEs of supported MoS_2 was close to 100%, indicating the complete conversion of phospholipids. Increasing the transesterification temperature also increases the energies of the substrates and catalysts and, thus, more collisions between the catalysts and substrates are expected to occur, which increases the mass transfer efficiency and reaction rate.[27] When the temperature exceeds 60 °C, the yield of FAMEs did not increase further. Therefore, the optimal reaction temperature was confirmed to be 50 °C.

3.5 Catalytic mechanism

The possible catalytic mechanism of the transesterification reaction between lecithin and methanol is illustrated in Fig. 9. Methanol would be deprotonated to form a methoxy anion in the presence of sodium carbonate, which acted as a nucleophile to attack the carbonyl C atom of two fatty acid chains of lecithin to generate FAMEs and the byproduct glycerophospholipids (GPX).

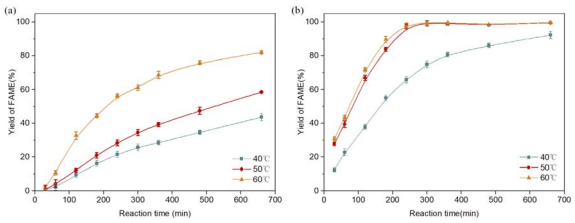

Fig. 8 Effects of reaction temperature on the transesterification reaction (a) for the catalyst of 1 mg of unsupported Na_2CO_3 and (b) for the catalyst of 5 mg of 20%-Na_2CO_3 supported MoS_2. Reaction conditions: 10 mg of lecithin dissolved in 20 mL of methanol, 50 °C with a stirring speed of 500 rpm.

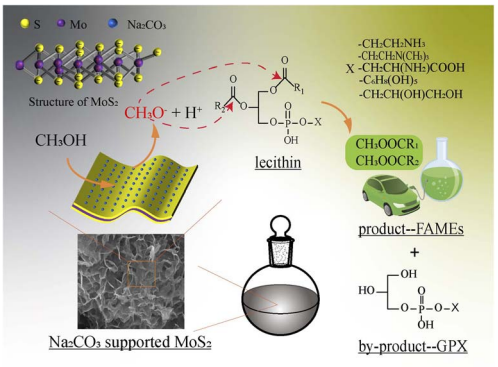

Fig. 9 A schematic diagram of the transesterification reaction between lecithin and methanol.

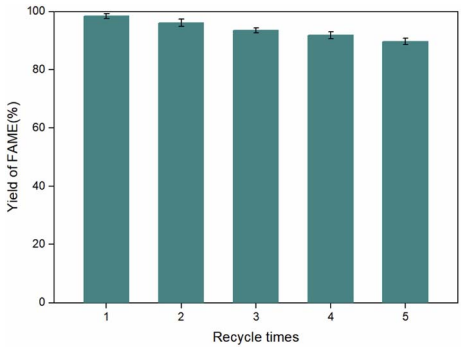

Fig. 10 Recycling test of 20%-Na_2CO_3 supported MoS_2 catalyst over five cycles.

GPX with different polar head groups are a kind of water-soluble phospholipid, which are easily removed after the reaction.

MoS_2 alone also showed unignorable catalytic activity during the transesterification. This might be explained by the electron-rich properties of the unique layered nanostructure of MoS_2. Since MoS_2 was always used as a photocatalyst, the transesterification rate of MoS_2 under completely dark conditions was carried out. The yields of FAMEs were completely coincident with those in light conditions (the conversion profile was the same as the blue line in Fig. 7). Thus, the participation of active free radicals was excluded during the reaction.[28] The most important active intermediate in the transesterification reaction is the methoxy anion. The electron-rich outer layer of MoS_2 might promote the deprotonation of methanol to form active methoxy anions. Then, the active methoxy anion attacked the carbonyl carbon to form an intermediate product, and, finally, the target product was generated.

As shown in Fig. 7, the yields of FAMEs were greatly improved when catalyzed by the supported catalysts, indicating that there is a synergistic effect between MoS_2 and Na_2CO_3 in the transesterification of lecithin and methanol. The effective specific surface area and the dispersion in methanol of the sodium carbonate were greatly increased by the immobilization on MoS_2, which were beneficial to the collisions between sodium carbonate and methanol to generate the active methoxy anion groups. Moreover, the diffusion of negatively charged methoxy anions would be accelerated by MoS_2.[24] As a result, the transesterification rate between lecithin and methanol was enhanced substantially. It is worth noting that the synergy not only had a positive effect on the generation of the methoxy anion, but also promoted the diffusion of the substrates. The main component of lecithin was PC, which has a polar head group (choline) with positive charges and would, thus, prefer to attach to the electron-rich surfaces of MoS_2. Then, these adsorbed PC molecules would act as anchor molecules to further attract other phospholipids (such as PE, and PI) by the hydrophobic interaction.[29]

3.6 Reusability and stability of the catalysts

The possibility of recovering and reusing heterogeneous catalysts is an important issue for the chemical industry. In the present work, the reusability and stability of 20%-Na_2CO_3 supported MoS_2 were investigated systematically. The catalysts were re-used for five cycles using a simple rinse without any further purification and activation. After each run, the catalyst was separated from the reaction mixture by centrifugation and re-used in the consecutive run with fresh portions of lecithin and methanol. As shown in Fig. 10, the catalytic performance of Na_2CO_3 supported MoS_2 did not exhibit a significant decrease during five cycles, with FAMEs yields of 98.4%, 96.1%, 93.5%, 91.8%, and 89.7%. A slight and isocratic decrease in the FAME yield was observed after each cycle, due to the physical loss of the catalyst during recycling times and centrifugation. Moreover, the slight leakage of Na_2CO_3 is another reason for the activity loss of supported MoS_2.[30] The former has very slight solubility in an excess of methanol and methanol/glycerol solutions.[21] After each run, the remaining liquid phase was collected after filtering the solid phase and washing with *n*-hexane several times until no FAMEs were detected. Next, fresh lecithin was added to test the leakage of Na_2CO_3.[31] The yield of FAMEs was less than 3% after 12 hours of transesterification, showing that the leaching of Na_2CO_3 was negligible.[3] The S-rich surface and some dangling bonds of the MoS_2 can be complexed with some ions or molecules,[26] thus, MoS_2 exhibits appealing adsorption to sodium carbonate, which reduces the possibility of the leakage of sodium carbonate. XRD was used to examine the crystallinity of the catalysts before and after

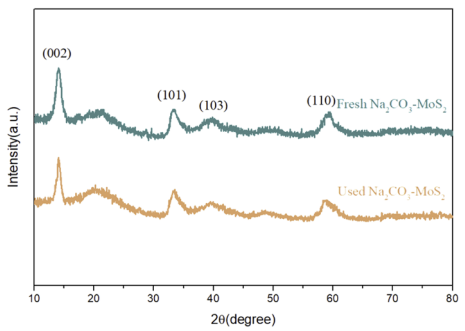

Fig. 11 XRD patterns of fresh Na_2CO_3-supported MoS_2 and used Na_2CO_3-supported MoS_2.

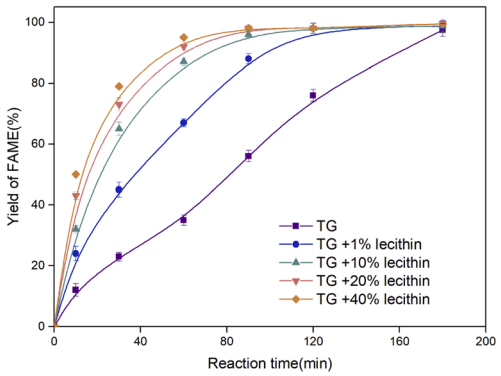

Fig. 12 Effects of different lecithin content levels on the transesterification reaction; reaction conditions: x (x = 0, 1, 10, 20, 40) mg of lecithin dissolved in 100 mg of TG, 200 mL of methanol, 20 mg of 20%-Na_2CO_3 supported MoS_2 catalyst, 50 °C, a stirring speed of 500 rpm.

recycling, as shown in Fig. 11. The XRD patterns did not show a significant change, indicating the excellent stability of the prepared catalytic matrix.

3.7 Application of high-phospholipid-content oil to prepare FAMEs

Oils derived from animal, plant, and microbial cells often contain a certain amount of phospholipids, while those derived from waste cooking oil have a higher content of up to about 40% of phospholipids.[32] Sodium carbonate supported MoS_2 has been demonstrated to show excellent catalytic activity for the transesterification of lecithin with methanol. Therefore, 20%-Na_2CO_3 supported MoS_2 was used to further catalyze triglycerides (TG) with different lecithin contents (1%, 10%, 20%, and 40%), as shown in Fig. 12.

The yields of FAMEs were close to 100% for all feedstocks. The transesterification rate increased with the content of lecithin, demonstrating that the supported catalysts were promising candidates for biodiesel production from crude oil with high viscosity or high gum levels. It benefited from the amphiphilic properties of lecithin, enabling lecithin to easily interact with and attach onto the polar catalyst. Meanwhile, these adsorbed lecithin molecules would act as anchor molecules to further attract triglycerides by a hydrophobic interaction through their hydrophobic fatty acid tails.[29] Therefore, in the present work, lecithin acted as a critical substance that could not only be converted into FAMEs, but also promote the transesterification efficiency of the biodiesel production.

4. Conclusions

In this paper, the effects of 23 kinds of alkaline salts with different anions and cations on the transesterification of lecithin were investigated, and the results showed that sodium carbonate was the best candidate. Then, sodium carbonate was loaded on the nanosheet surface of hierarchical MoS_2 nanosheets. The activity performance of the supported catalysts was evaluated during transesterification. The results showed that 20% Na_2CO_3 supported MoS_2 exhibited the highest catalytic efficiency. The maximum yield of FAMEs was close to 100% under mild conditions (50 °C, 500 rpm) with 5 mg of supported catalyst (containing 1 mg of Na_2CO_3 and 4 mg of MoS_2). The specific activity was 40.58 ± 0.78 U $(mg_{Na_2CO_3})^{-1}$, which is 2.43 times higher than that of unsupported sodium carbonate. Synergy between the electron-rich surface of MoS_2 and absorbed sodium carbonate was deduced to promote the deprotonation of methanol to generate a high concentration of methoxy anions, which attacked the carbonyl carbon atoms of lecithin to form fatty acid methyl esters. The supported catalyst was then applied in the transesterification of lecithin-containing triglycerides, and a positive influence was shown upon the addition of lecithin. It can be concluded that TG containing elevated levels of lipids can be used for transesterification without degumming. Hence, the supported catalysts are promising candidates for biodiesel production from crude oil because of their excellent catalytic performance, the mild reaction conditions required, and the noticeable reusability.

Conflicts of interest

There are no conflicts to declare.

Acknowledgements

We are thankful for funding from the Key Research and Invention Program in Shaanxi Province of China, grant/award number: 2020NY-127; the Shaanxi Association for Science and Technology for Young Scholars, grant number: 20220201; the National Natural Science Foundation of China for Young Scholars, grant/award number: 22108227; and the Science and Technology Program for Young Scholars in Gansu Province of China, grant/award number: 20JR5RA484.

Notes and references

1 S. Kanakraj and S. Dixit, *Biofuels*, 2016, **7**, 537–548.
2 X. Fan, R. Burton and G. Austic, *Int. J. Green Energy*, 2010, **7**, 593–599.
3 A. L. de Lima, C. M. Ronconi and C. J. A. Mota, *Catal. Sci. Technol.*, 2016, **6**, 2877–2891.
4 D. M. Reinoso, D. E. Damiani and G. M. Tonetto, *Catal. Sci. Technol.*, 2014, **4**, 1803–1812.
5 H. Zhang, L.-L. Zhang, X. Tan, H. Li and S. Yang, *Ind. Crops Prod.*, 2021, **173**, 114126.
6 H. Kuramochi, Z. Zhang, K. Yui, T. Kobayashi and K. Maeda, *Fuel*, 2020, **263**, 116600.
7 X. Tan, H. Zhang, H. Li and S. Yang, *Fuel*, 2022, **310**, 122273.
8 I. M. Atadashi, M. K. Aroua and A. A. Aziz, *Renewable Sustainable Energy Rev.*, 2010, **14**, 1999–2008.
9 H. Zhang, H. Li, Y. Hu, K. T. V. Rao, C. Xu and S. Yang, *Renewable Sustainable Energy Rev.*, 2019, **114**, 109296.
10 R. K. Balasubramanian and J. P. Obbard, *Bioresour. Technol.*, 2011, **102**, 1942–1946.
11 K. Malins, *Fuel Process. Technol.*, 2018, **179**, 302–312.

12 S. L. Britton, J. Q. Bond and T. W. Root, *Energy Fuels*, 2010, **24**, 4095–4096.
13 M. E. Martínez-Klimov, P. Ramírez-Vidal, P. Roquero Tejeda and T. E. Klimova, *Catal. Today*, 2020, **353**, 119–125.
14 K. Wilson and A. F. Lee, *Catal. Sci. Technol.*, 2012, **2**, 884.
15 Y. Li, R. Fu, Z. Duan, C. Zhu and D. Fan, *Adv. Healthcare Mater.*, 2021, **11**, 2101849.
16 D. Wang, M. Guo, J. Li, B. Li and J. Wang, *Biotechnol. Prog.*, 2022, e3256, DOI: **10.1002/btpr.3256**.
17 Y. Zhang, L. Zhu, G. Wu, X. Wang, Q. Jin, X. Qi and H. Zhang, *LWT*, 2022, **154**, 112635.
18 F. D. Gunstone, F. B. Padley and J. L. Harwood, *The Lipid Handbook*, London, 1994.
19 V. V. Patil, R. V. Galge and B. N. Thorat, *Sep. Purif. Technol.*, 2010, **75**, 138–144.
20 R. D. Jangle, V. P. Magar and B. N. Thorat, *Sep. Purif. Technol.*, 2013, **102**, 187–195.
21 A. Platonov, A. Evdokimov, A. Kurzin and H. Maiyorova, *J. Chem. Eng. Data*, 2002, **47**, 1175–1176.
22 J. Li, C. Zhang, H. Ma, T. Wang, Z. Guo, Y. Yang, Y. Wang and H. Ma, *Chem. Eng. J.*, 2021, **414**, 128834.
23 N. Qureshi, S. Arbuj, M. Shinde, S. Rane, M. Kulkarni, D. Amalnerkar and H. Lee, *Nano Convergence*, 2017, **4**, 25.
24 X. Li, W. Zhang, Z. Liu, S. Wang, X. Zhang, B. Xu, P. Yu, Y. Xu and Y. Sun, *Sep. Purif. Technol.*, 2022, **294**, 121139.
25 E. Garousi, M. H. Sadr, A. Rashidi and M. Yousefi, *Inorg. Chem. Commun.*, 2022, **138**, 109223.
26 N. Thomas, S. Mathew, K. M. Nair, K. O'Dowd, P. Forouzandeh, A. Goswami, G. McGranaghan and S. C. Pillai, *Mater. Today Sustain.*, 2021, **13**, 100073.
27 A. V. Metre and K. Nath, *Pol. J. Chem. Technol.*, 2015, **17**, 88–96.
28 W. Huang, Y. Li, Q. Fu and M. Chen, *Mater. Res. Bull.*, 2022, **147**, 111650.
29 X. Zhang, B. Li, J. Wang, H. Li and B. Zhao, *J. Agric. Food Chem.*, 2017, **65**, 10767–10774.
30 N. Kaur and A. Ali, *Fuel Process. Technol.*, 2014, **119**, 173–184.
31 D. Meloni, R. Monaci, Z. Zedde, M. G. Cutrufello, S. Fiorilli and I. Ferino, *Appl. Catal., B*, 2011, **102**, 505–514.
32 P. M. Foley, E. S. Beach and J. B. Zimmerman, *Green Chem.*, 2011, **13**, 1399–1405.